Journal of Coastal Conservation (2021) 25: 1
https://doi.org/10.1007/s11852-020-00788-y

Tropical cyclone risk mapping for a coastal city using geospatial techniques

Aysha Akter[1] · Ahammed Dayem[1]

Received: 9 December 2019 / Revised: 4 December 2020 / Accepted: 8 December 2020 / Published online: 8 January 2021

Abstract

Tropical cyclone associated storm surges and their disastrous influences are becoming a major concern amongst the worldwide coastal community. The detailed risk modelling study seems an urgent need to support the storm surge mitigation actions. Using a Geographic Information System (GIS) based risk model, this study attempted to obtain both present and future storm surge wave heights in the Cox's Bazar Sadar Upazilla in Bangladesh. Linear storm surge model setup was done for the different return periods includes 5, 10, 20, 50, and 100 years. Also, to assess climate change effects, a 0.34 m sea-level rise in 2050 was tested using the regional scale surge models. The simulated storm surge model provided a time series dataset for the risk model and obtained risk maps comprised of the relationship among risk zone and the return periods. With the present inundation depth trend, the acquired risk maps of 50 and 100 year return period showed that 10.13% and 36.4% of the study area belongs to very high-risk zone respectively. Conversely, for future inundation depth conditions 30.83% and 49.9% of the study area would be within a very high-risk zone in 50 and 100 year return period respectively. This is envisaged that a detailed historical inundation dataset could enrich the adopted approach considering both present and future storm surge risk modelling for the Decision Support System (DSS). Also, this approach might be adopted for other identical coastal environments to aid mitigation programs and strategies.

Keywords Storm surge · Model · Coastal environment · Inundation · Risk zone

Introduction

Coastal areas are experienced with tropical cyclones as the most hazardous as well as destructive coastal hydro-meteorological hazards. Land-falling tropical cyclones usually appear with strong winds, higher storm surges, and heavy rainfall, thus, cause both tangible and intangible losses (Kumar et al. 2011; Li and Li 2013; Brammer 2016). As a consequence, many of the coastal areas throughout the world experience hardships rather regular basis, sometimes even with higher frequency (Peduzzi et al. 2012; Hoque et al. 2017a, b). Usually, significant tropical cyclones generate storm surges on the coastal cities with destructive forces. During 1970–2010, about 637 significant tropical cyclones were recorded around the world i.e. 88 tropical cyclones experienced per year (Shultz et al. 2005; Weinkle et al. 2012). In every three years, on average, a severe cyclone strikes Bangladesh and often proper remedial measures fail to minimize the sufferings (Dasgupta et al. 2009). Since 1970, Bangladesh has experienced 36 cyclonic storms that caused over 450,000 deaths along with intangible losses. Coastal embankments protected these areas gradually lessen coverage for the whole area due to increased frequency and cyclonic storm surges. Thus, the wave (surge plus tide) frequency of 10 m and 7 m might experience once per 20 years and 5 years respectively (Khan 1991). However, these cyclones strike almost every year either in April–May or October–November. Usually, a tropical cyclone generated within the Bay of Bengal continues for a particular week to prolonged time. Forming wave propagated through the shallower inland coastal areas and the associated wave heights increase due to shallow water effect. Researchers highlighted climate change effects on the worldwide tropical cyclone activities viz. cyclone strength and rate of recurrence of cyclones (Karim and Mimura 2008; Mendelsohn et al. 2011). Thus, without proper prediction tropical cyclone catastrophes would be difficult to minimize in cyclone prone developing

✉ Aysha Akter
aysha_akter@cuet.ac.bd; http://aakter.weebly.com

[1] Department of Civil Engineering, Chittagong University of Engineering & Technology (CUET), Chittagong 4349, Bangladesh

countries. In this connection, risk modelling showed better performance with cyclone disaster prediction as well as the mitigation/management action. These models deal with the spatial risks, key infrastructures, and risk prone community as well as responsible risk factors (Li and Li 2013; Fang et al. 2016).

In addition to these, scenario-based potential hazards maps and their resulting vulnerability could aid successful risk modelling (Gambolati et al. 2002; Dewan et al. 2007; Condon and Sheng 2011; Masood and Takeuchi 2011; Darsan et al. 2013; Thompson and Frazier 2014), and mapping to improve future mitigation programs and approaches. Thus, details on the locations and numbers of cyclone shelters could be offered to wellbeing for the vulnerable community (Shutler et al. 2016). To feature detailed cyclone risks with basic insight, various types of modelling software and also Geographic Information System (GIS) based applications are used in the available disaster risk models. Digital Elevation Model (DEM) incorporated within the storm surge model setup (Gambolati et al. 2002; Puotinen 2007; Karim and Mimura 2008; Condon and Sheng 2011; Darsan et al. 2013; Li et al. 2016). These risk models usually include both existing and projected population, land use, and land cover for the hazard and vulnerability analysis (Darsan et al. 2013). On the other hand, storm surge modelling software is generally based on advanced programming language skills and extensive meteorological datasets (Dasgupta et al. 2009; Condon and Sheng 2011; Lewis et al. 2012). Furthermore, comprehensive local level risk details are required to determine risk type as well as to identify the best mitigation option. Accordingly, even a simple modelling strategy at local scales, for instance, 1 to 5 km or an area of <1000 km^2 could offer detailed risk insights (Karim and Mimura 2008). Thus, GIS and Remote Sensing (RS) techniques have been widely practiced for cyclone risk modelling due to its simplicity and effectiveness (Puotinen 2007; Darsan et al. 2013; Fang et al. 2016). To enrich geospatial-based risk modelling, the expected surges from tropical cyclones are featuring as a combined outcome of sea-level rise due to climate change (Emad et al. 2010; Saxena et al. 2012; Thompson and Frazier 2014; Fang et al. 2016). Consequently, this is necessary to evaluate the climate change effects by incorporating sea-level rise in the risk modelling procedure as the available literatures on storm-surge risk modelling are limited to advanced hydrodynamic model usage (Karim and Mimura 2008; Emad et al. 2010; Condon and Sheng 2011). Moreover, regional sea level rise can be modelled for geospatial based risk analysis (Fang et al. 2016).

This reported study focused on a risk prediction tool considering present and future climate conditions at local scales. This study aimed to develop a geospatial risk modelling approach considering present and future surge wave height on Cox's Bazar Sadar Upazilla, Bangladesh.

Materials and method

In this research, during the storm surge model setup, a geospatial strategy was applied using the Gumbel distribution method for a range of return periods. So far, this is the well-practiced probability distribution method for frequency analysis (Stedinger et al. 1993; Hoque et al. 2017a, b). To evaluate the climate changes, the local or regional sea-level rise was tested in these surge models. Then, population density within the study area was incorporated during hazard, vulnerability, and risk assessment. Prior to this, maps were generated for different return periods, inundation depths, population density and the vulnerability due to floods. Inundation depths were calculated from the surge model using DEM data and flow processing (Fig. 2). This study covered the Cox's Bazar Sadar Upazilla of 228.23 km^2 (between 21°24′ N and 21°36′ N latitudes and between 91°59′ E and 92°08′ E longitudes) in the southeastern coast of Bangladesh (Figs. 1 and 2). The term "Upazilla" represents the third local governmental administration sector in Bangladesh. During the last century, around 508 tropical cyclones were recorded in the Bay of Bengal (Paul et al. 2016). The study area is located adjacent to the Bay of Bengal, bordered by Ramu Upazila in the south and east, Chakaria Upazila existed in north and Maheshkhali Upazilla in the west. This reported study comprises of both primary and secondary datasets (Table 1). Fieldwork was conducted using a Laser Distance Meter and a Geographic Positioning System (GPS), to collect cyclone Mora's 2017 landfall extents for the model validation. To verify accumulated land cover and land use maps, point-based reference data were collected. Additionally, spatial data were gathered from NASA (Table 1). In the geospatial analysis, World Geodetic System (WGS)-1984 datum including the Universal Transverse Mercator (UTM) zone 46 north was selected as a geographic reference. Information on population migration, wave condition, and changing frequencies during cyclones was ignored during this research.

Surge model study

Storm surge inundation depth was taken into consideration as linearly decaying on the way to the inland. Based on the available researches (Hoque et al. 1996; Swinkels et al. 2009), the formulated hypothesis was a constant surge wave height to a certain distance with or without dykes and subsequently, this height linearly decreased to the overall inundation extends. Previous cyclone data including surge heights for different return periods were used to determine Surge Decay Coefficient (SDC) (Table 2). Storm surge scenarios along with the SDC values were applied with DEM data within ArcGIS software.

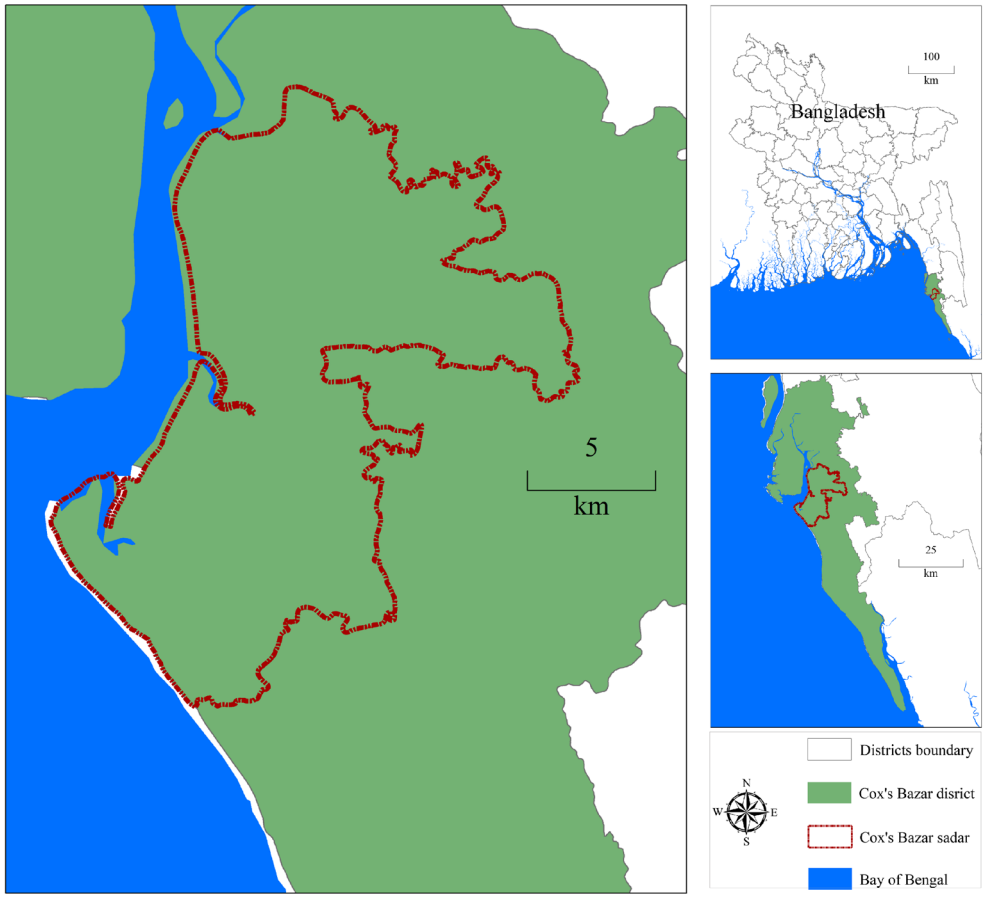

Fig. 1 **a** Bangladesh map. **b** District map of Cox's Bazar. **c** Cox's Bazar Sadar Upazilla

Surge height frequency analysis

From 1963 to 2017, the south-eastern coastal region of Bangladesh has experienced 12 storm surges (Table 2). Surge heights frequency analysis was carried for the different return periods i.e. 5 year, 10 year, 20 year, 50 year, and 100 year using the Gumbel distribution method for the historical cyclone dataset (i.e., 1963–2017). An equation following Benson (1962), was developed for estimating surge height (Y) in different return periods (X) (Fig. 3). Thus, the calculated extreme surge heights for the return periods of 5 year, 10 year, 20 year, 50 year and 100 year were 4 m, 4.8 m, 5.8 m, 7 m, and 7.8 m respectively.

Tropical cyclone

In the coastal areas, sea-level rise is a great concern. If future sea-level rise happens, tropical cyclones might be associated with higher storm surge floods (Ward et al. 2011). Usually, complex interactions within the local, regional, global land, and oceanic processes are considered for projecting sea-level changes. The local sea-level rise of 0.34 m was selected following the earlier researchers (Dasgupta et al. 2014; Hoque et al. 2017a, b) to assess future storm surge inundations due to tropical cyclones.

Model setup

For model setup, 12.5 m DEM data was acquired from the NASA earth data and a tree height offsets estimation technique was adopted following Gallant et al. (Gallant et al. 2012). Afterward, the DEM data was prepared to reduce associated errors by interpolating points in the ArcGIS environment. Before the surge model simulation, surge depth was calculated following the earlier mentioned strategies for the SDC. Here, the SDC is considered as a function of the friction due to land use and land cover (Fig. 4).

$$SDC = \frac{\text{surgeheight} - \text{average elevation at the end of surge}}{\text{totalinundationwidth} - \text{width of constantsurge}} \quad (1)$$

An equation was developed based on the relation between average inundated height and area for the entire coast of Bangladesh (Damen and Van Westen 1995). Constant surge area at a distance from the coast (D) was calculated, and, Y is the surge height (Figs. 5 and 6) due to cyclone Mora 2017 in this area. Then, the calculated extreme surge heights 4 m, 4.8 m, 5.8 m, 7 m, and 7.8 m, were verified for the return

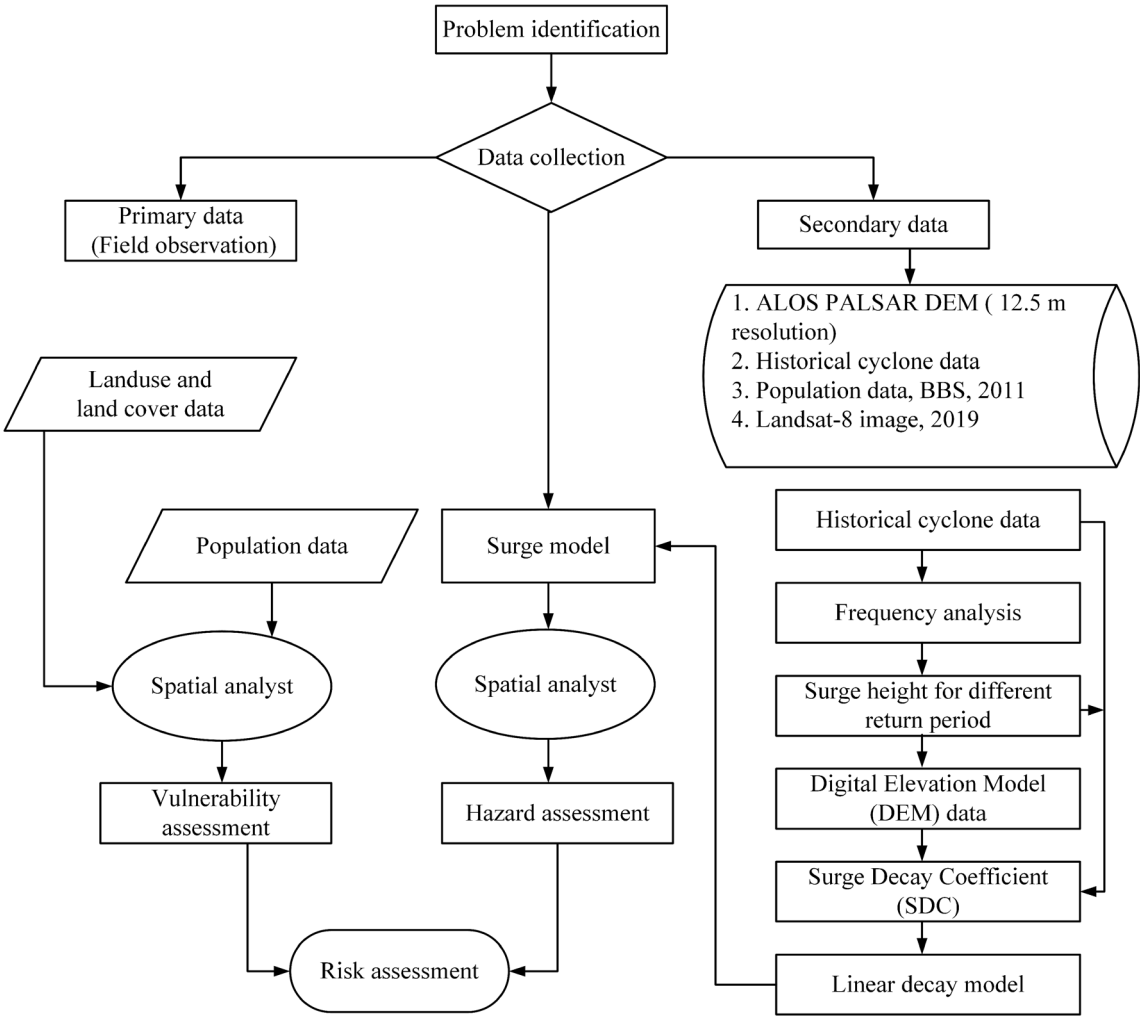

Fig. 2 Adopted method in this study

periods of 5 year, 10 year, 20 year, 50 year, and 100 years respectively.

In this study, the total inundation widths for numerous surge levels were acquired from the particular field inundation magnitude of tropical cyclone 1991 and Mora cyclone 2017. Additionally, local sea-level rise of 0.34 m was tested for different surge heights for existing conditions and SDC values. Numerous raster calculator formulas were applied in the storm surge model setup for different return periods using ArcGIS based on the SDC values and bare-earth DEM. In addition to this, cyclone landfall scenarios were also considered Table 3.

Hazard assessment

Hazards are described as incidents, usually, function as a likely danger to life, real estate, and the natural environment. In the hazard evaluation process, outcomes are greatly

Table 1 Details on input dataset

Application	Data type	Source	Period
Storm-surge modeling	ALOS PALSAR-DEM (12.5 m resolution)	NASA Earth Data	3 February 2019
Population density	Population	Bangladesh Bureau of Statistics (BBS)	Population Census 2011
Frequency analysis	Historical cyclone	Cyclone hazard in Bangladesh (Khan 1991) and others	1963–2017
Surge decay calculation	Cyclone inundation extent	Modelling cyclone hazard in Bangladesh (Damen and Van Westen 1995) and tropical cyclone Mora 2017	

Table 2 List of significant tropical cyclones storm surge that hit in the southeastern coastal region of Bangladesh (1963–2017) (Khan 1991)

Sl No	Date of occurrence	Landfall area	Maximum wind speed (km/h)	Maximum surge height (m)	Loss
1	28–29 May 1963	Chittagong to Cox's Bazar Coast	201	5	11,520 people were died
2	14–15 Dec 1965	Cox's Bazar to Teknaf Coast	200	4	40,000 salts belts inundated and 840 people were died
3	23–24 Oct 1967	Chittagong to Cox's Bazar	130	2	128 people were died
4	5–7 May 1970	Chittagong to Teknaf Coast	148	2.3	18 people were died
5	24–28 Nov 1974	Cox's Bazar to Chittagong coast	161	3.1	20 people were died
6	09 Nov 1983	Chittagong to Teknaf Coast	136	2.5	300 fishermen were missed with 50 boat, 200 houses were damaged, 22 institutions were destroyed
7	24–25 May 1985	Noakhali to Cox's Bazar coast	154	3.2	11,069 people were died, 94,379 houses damaged, 390 km embankment damaged.
8	29 Apr 1991	Patuakhali to Cox Bazar	235	5.8	1 45,000 people were died, 70,000 cattle killed, crops were damaged.
9	16–19 May 1997	Cox's Bazar	225	3.05	126 people were died
10	25–27 Sep 1997	Cox's Bazar	150	3.05	No data available
11	16–20 May 1998	Cox's Bazar	150	2.44	No data available
12	29–31 May 2017	Cox's Bazar	110	2.03	20,000 houses damaged in refugee camps.

influenced by the storm surge wave height for individual return periods (Shepard et al. 2012; Li and Li 2013). Thus, the inundation depths for the different return periods were acquired from adopting storm surge models and were featured on hazard maps. In this connection, classifications of hazards for the inundation depth were adapted from Hoque et al. (2017b).

Vulnerability assessment

The 'vulnerability' is the degree of damage due to hazard to the components that are at just risk includes the built environment, human resources, and the natural environment. Here, this has been evaluated as the vulnerability to the adjacent community due to several return periods storm surge related inundation depths for both present and future model simulations. Vulnerability for any particular inundation depth was estimated following tropical cyclone Mora 2017 and relevant studies (Damen and Van Westen 1995; Hoque et al. 2017a, b). Then, following available researches, generated maps for the vulnerable area were categorized into five classes included very low, low, moderate, high, and very high (Table 4).

Risk assessment

Risk estimates the possibility of destruction due to the combined effects of vulnerability, hazards, and levels of exposure. Also, risks for a specific return period due to storm surge inundation are the statistical probabilities that might deliver the potentiality of a phenomenon (Gambolati, Teatini and Gonella, 2002). Here, the risk model for the storm surge in an affected community was evaluated as:

$$\text{Risk} = H_t \times V \times E \quad (2)$$

Here, H_t refers to the occurrence probability (hazard) at least once in due course, V represents the vulnerability (vulnerability to the community based on respected surge heights) and E is the exposure (i.e., population density, Fig. 7). Then, the risk maps were developed using probability, vulnerability maps, and exposure for the different return periods using ArcGIS. Risk evaluation was limited to the population growth rate rather than land-use properties for the different surge depths. The local population growth for different return periods was considered i.e. 0.72% per year following BBS (Based on BBS 2011).

Results and discussion

Model output (surge model)

By adopting the simple linear decay geospatial strategy, the surge model setup was done for the different return periods. During the calibration period, the local sea-level rise record

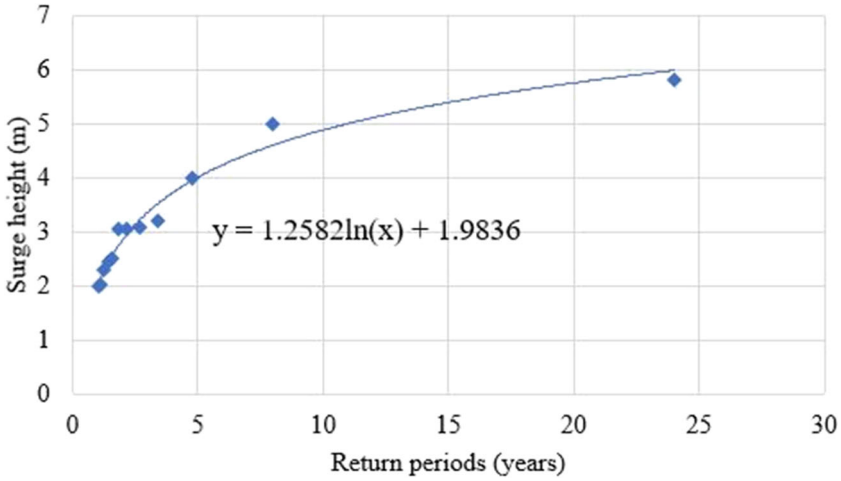

Fig. 3 Surge height calculation (Benson 1962)

was integrated with the present trend to project the condition in 2050 (Figs. 8 and 9). The surge model simulated inundation depth and extent generated map was validated by field survey including interviewing local personnel and relevant literature related to the inundation details.

Map generation for hazard assessment

The simulated inundation depths in the hazard maps were categorized into five hazard classes for both present trend and future conditions for the different return periods (Figs. 10 and 11). Following present climate condition, 22.62% of the study area exists between very low to low hazard zone and 77.38% (including very high 43.63%) moderate to very high hazard zone for the 50 year return period (Fig. 10). Compare to this, 19.11% of the area would remain in a very low to low hazard zone where 80.89% (including very high 44.47%) of the study area is within moderate to very high hazard zone for the 50 year return period at future climate condition (Fig. 11). Again the present climate trend simulated 14.60% spreads on very low to low hazard zone and 85.40% (including very high 58%) of the study area within the moderate to very high hazard zone for the 100 year return period. Conversely, based on the future climate condition the 100 year return period hazard map showed and 87.64% (including very high 64.54%) covers the moderate to very high hazard zone (Fig. 11).

Map generation for the vulnerability assessment

The vulnerability of the population in this area was evaluated and a map was generated for the different return period inundation depths in both future and present circumstances. The vulnerability map corresponding to the population and vulnerable areas were expanded with the increase of periods in both scenarios for different return periods (Figs. 12 and 13).

The obtained vulnerability map for 50 year return period in present trend showed 95.16% (including a very high 63.47%) area existed in the moderate vulnerable zone to very high with 4.84% very low to the low vulnerable zone. In comparison to

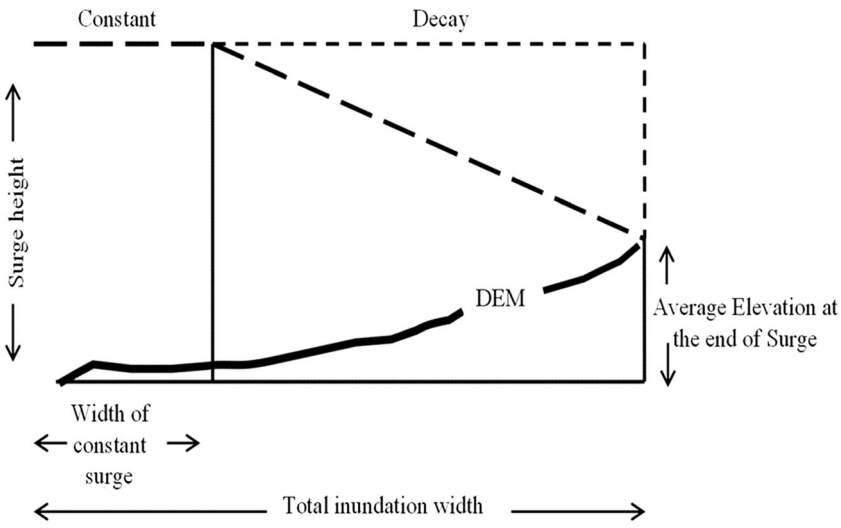

Fig. 4 Linear surge decay model setup schematic diagram (Hoque et al. 2017a, b)

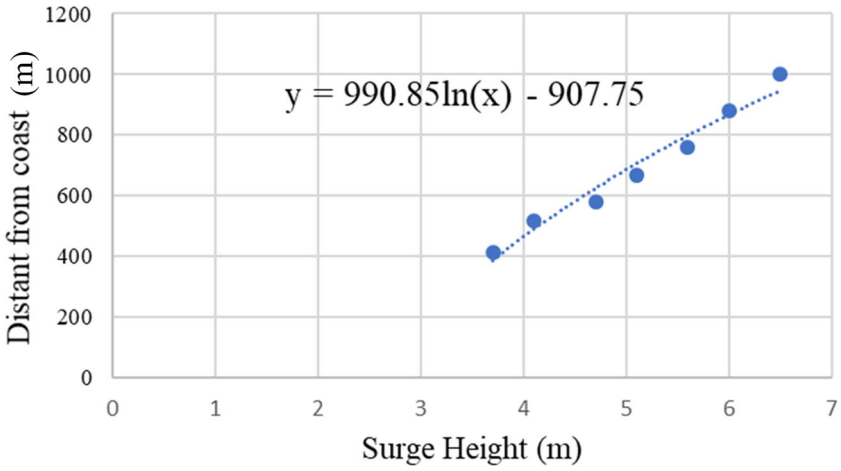

Fig. 5 Width of the constant surge

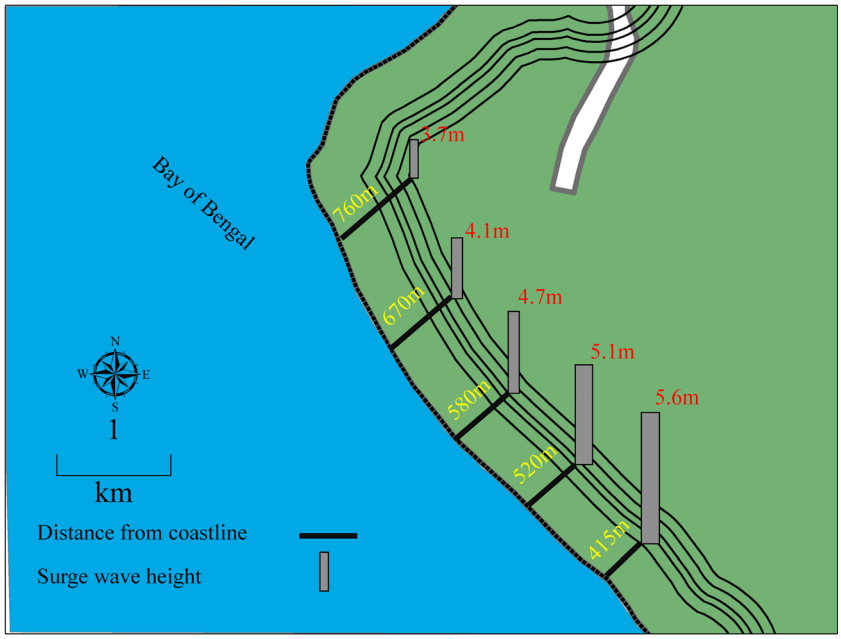

Fig. 6 Distance from the coastline for the constant surge wave height

future climate conditions, the resulting 50 year return period vulnerability map presented 95.96% (including very high 66.46%) of the study area within the moderate vulnerable zone to very high. Thus, present and future climate condition-based vulnerable maps showed 96% and 96.06% of the study area respectively would be within the moderate vulnerable zone to very high for the 100 year return period. Also, the vulnerability of land uses and land cover classes were simulated considering both climate scenarios for

Table 3 Assigned inundation depths ranges pertaining to hazard classes following Hoque et al. (2017a, b)

Inundation depths in m (surge heights)	Hazard classes
<0.5	Very low
0.5–1.5	Low
1.5–2.5	Moderate
2.5–3.5	High
>3.5	Very high

Table 4 Relationship between vulnerability and flood depth following researchers (Damen and Van Westen 1995; Hoque et al. 2017a, b)

Flood depth range (m)	Vulnerability
0.0	0.0
1.73	0.30
3.30	0.70
>=4.50	1.00

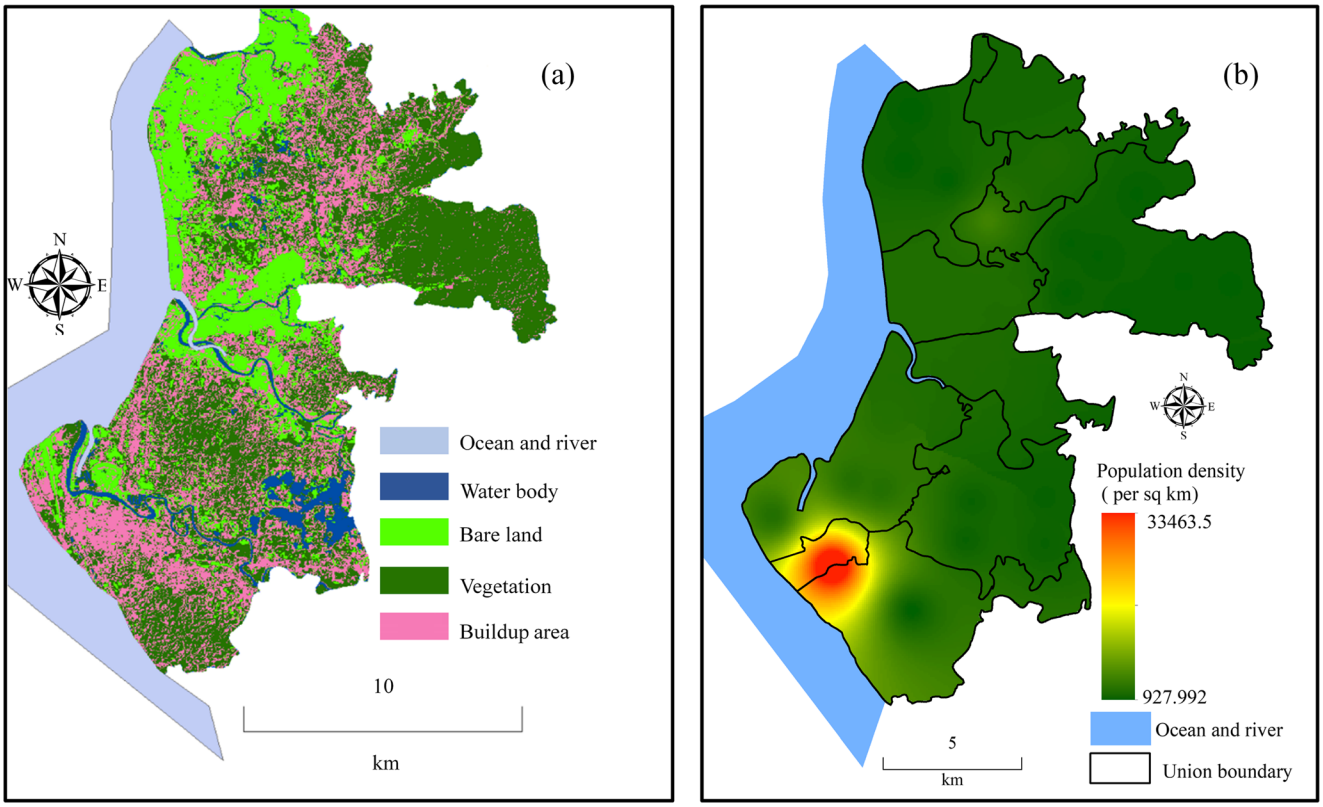

Fig. 7 **a** Land cover and land use map (Landsat-8 satellite image). **b** Population density map (Based on BBS 2011)

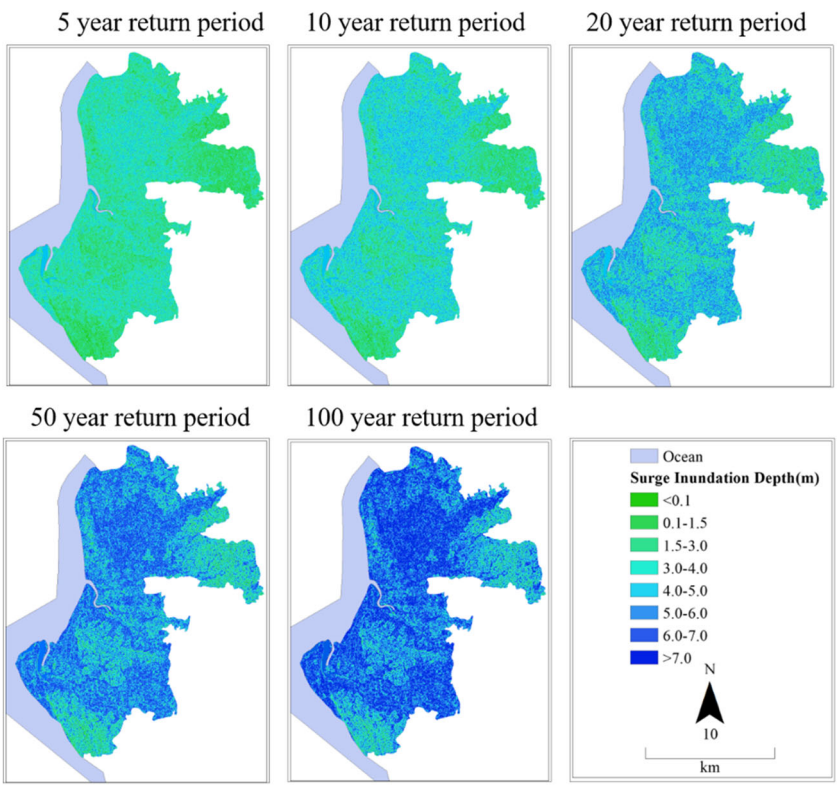

Fig. 8 Surge inundation depth following the present climate for the different return period

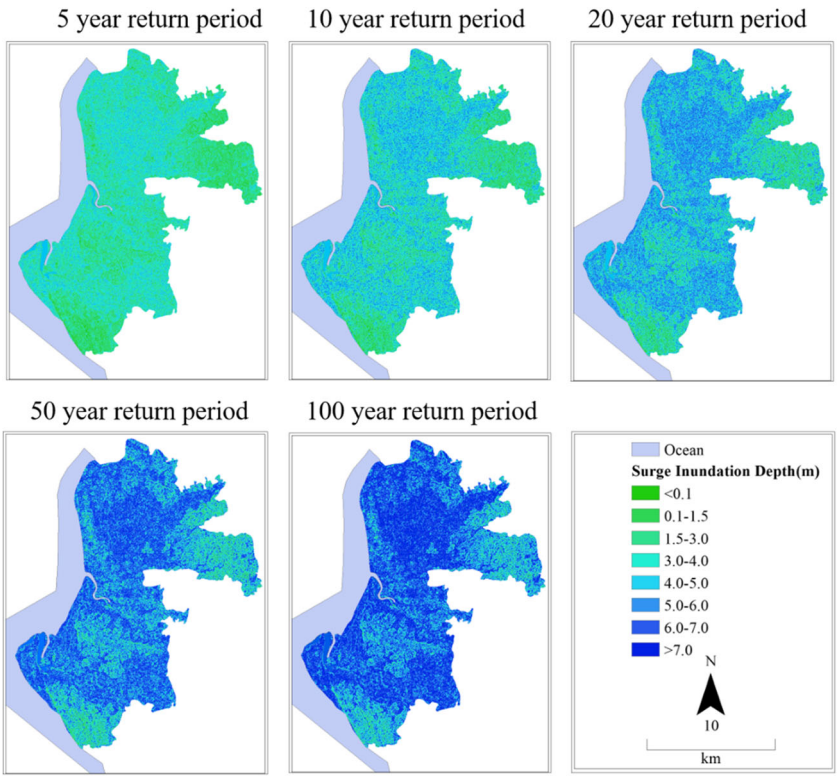

Fig. 9 Surge inundation depth due to sea-level rise 0.34 m for the different return periods (future climate condition)

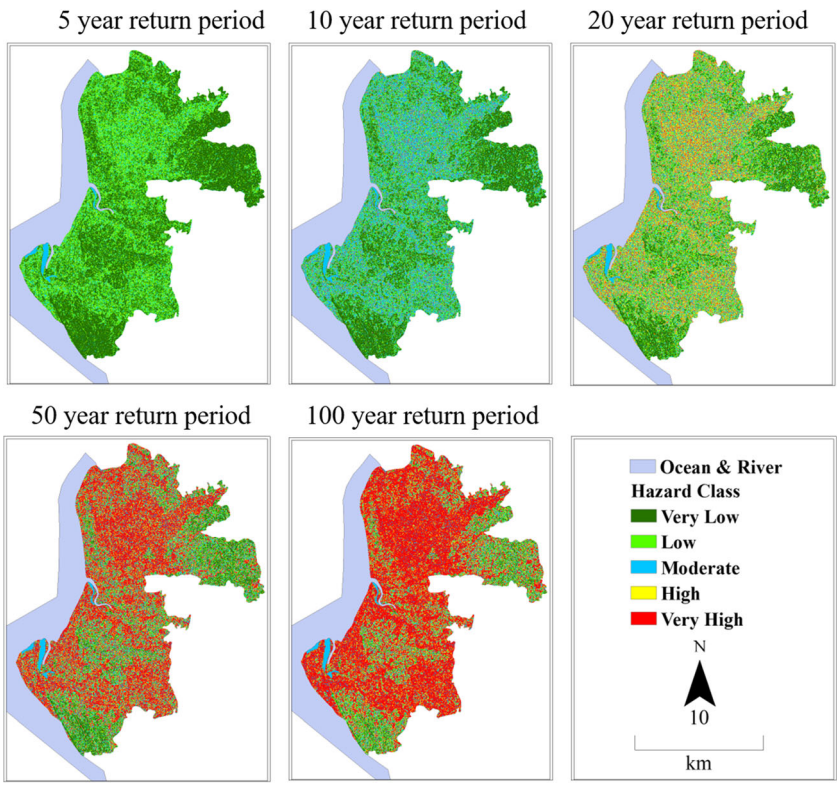

Fig. 10 Hazard maps for the different year return periods (present climate trend)

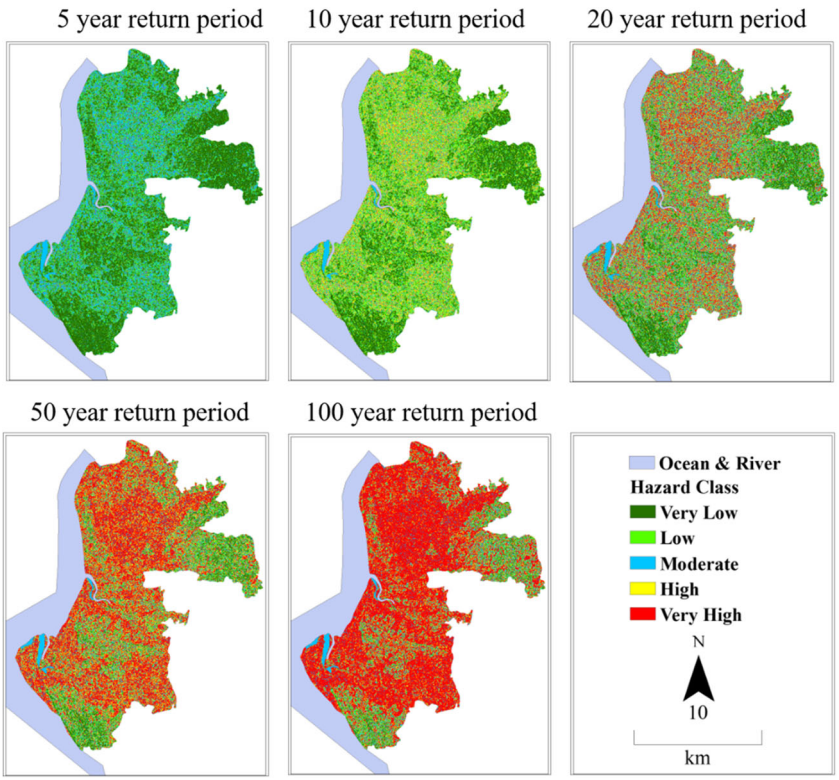

Fig. 11 Hazard maps for the different year return period at the future climate condition

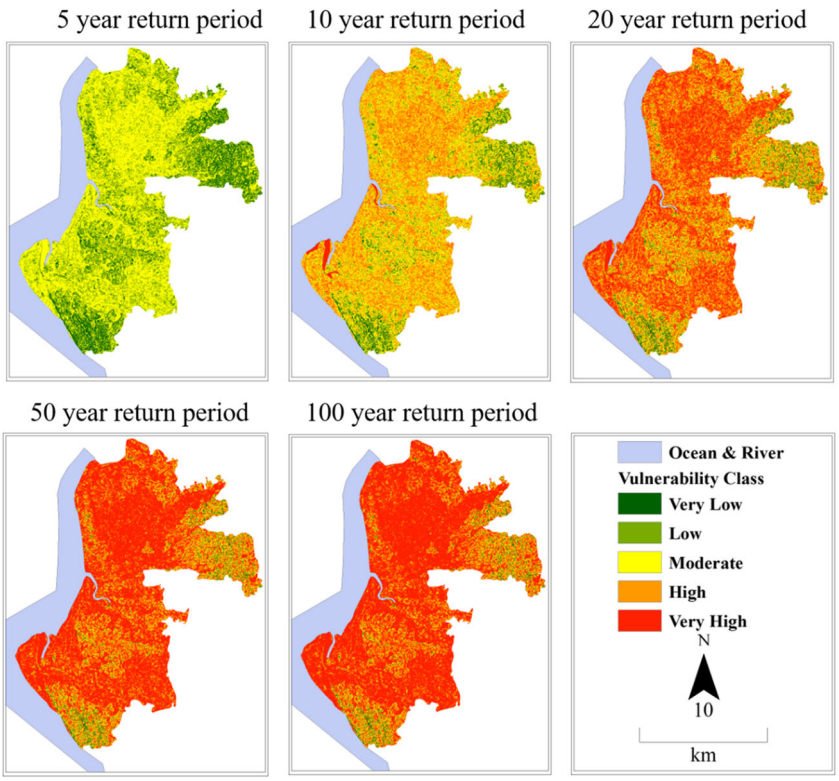

Fig. 12 Population vulnerability maps for the present climate trend

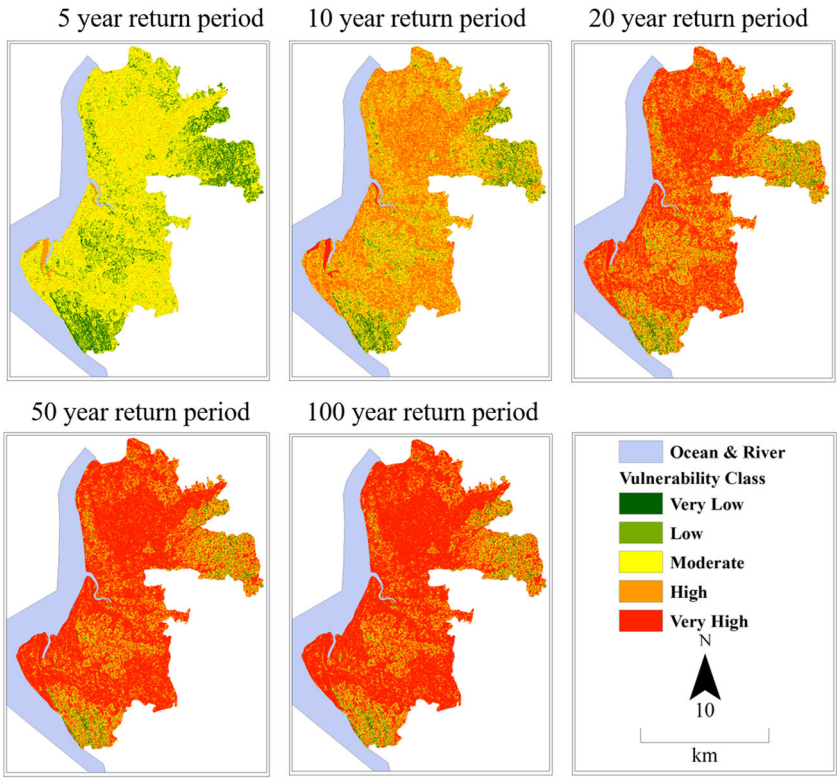

Fig. 13 Population vulnerability maps for the future climate

different storm surge inundation depth experiences greater than 1 m (Table 5).

Map generation for risk assessment

The generated risk map showed that the overall risk area increases corresponding to the population growth along with the increased return period surge event. The five classified levels were low to a very high-risk zone. Then, increased population density leads to a risk zone gradually, for instance, a very high-risk zone contains more population than the rest of the risk zone (Fig. 12).

The risk area is subjected to changes due to local mitigation measures including infrastructure establishment i.e. cyclone shelter and dykes. On the other hand, population growth, sea-level rise, and unplanned urbanization will increase the risk of flooding. 50 year return period risk map showed that presently 10.13% of the study area is prone to very high risk, with a 75% high-risk zone and so. Conversely, future climate condition shows that 30.83% of areas are at the very high-risk zone for 50 year return period. In the 100 year return period, 36.39% and 49.9% of the study area belong to the very high-risk zone in both present and future climate trends respectively

Table 5 Vulnerability of land cover and land use categories under >1.0 m storm surge flooding depth at baseline and climate change scenarios

	50 year return period				100 year return period			
Land use and Land cover	Present climate condition(km^2)	Affected area (%)	Future climate condition (km^2)	Affected area (%)	Present climate condition(km^2)	Affected area (%)	Future climate condition(km^2)	Affected area (%)
Water Body (9.31km^2)	9.15	98.28	9.18	98.60	9.2	98.82	9.22	99.03
Bare Land (49.2 km^2)	45.3	92.07	46.65	94.82	47.3	96.14	47.52	96.59
Vegetation (89.8 km^2)	82.6	91.98	83.52	93.01	84.63	94.24	84.96	94.61
Buildup area (61.36 km^2)	59.08	96.28	60.1	97.95	60.56	98.70	60.78	99.05

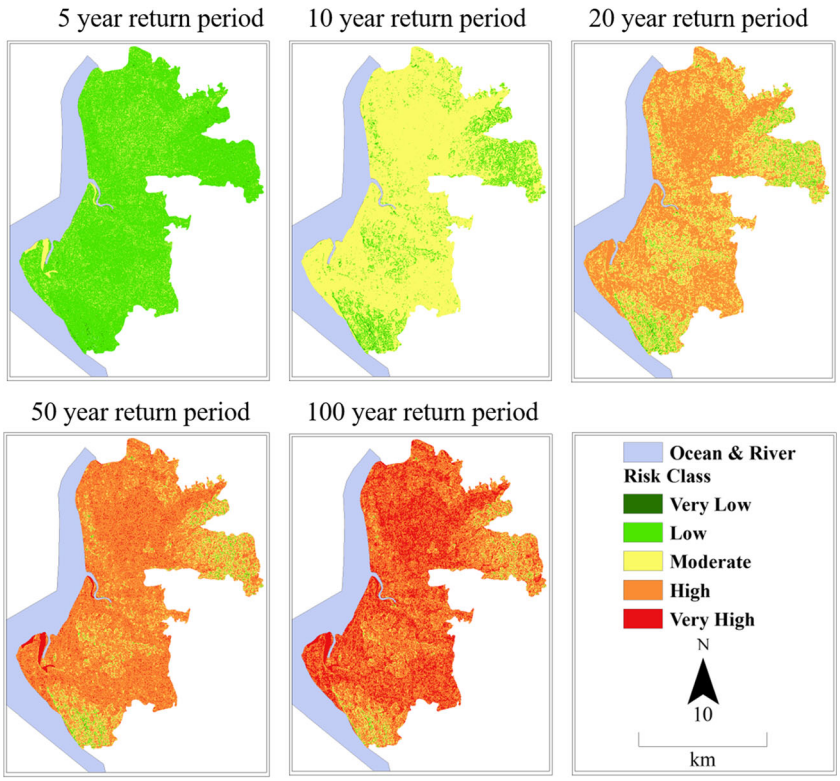

Fig. 14 Risk maps based on population for the present climate trend

(Figs. 13 and 14). Increasing risk area is significant for the future impact. Geographically few places seem out of risk, seaside but elevated these locations are in very low and low-risk zones (Fig. 15).

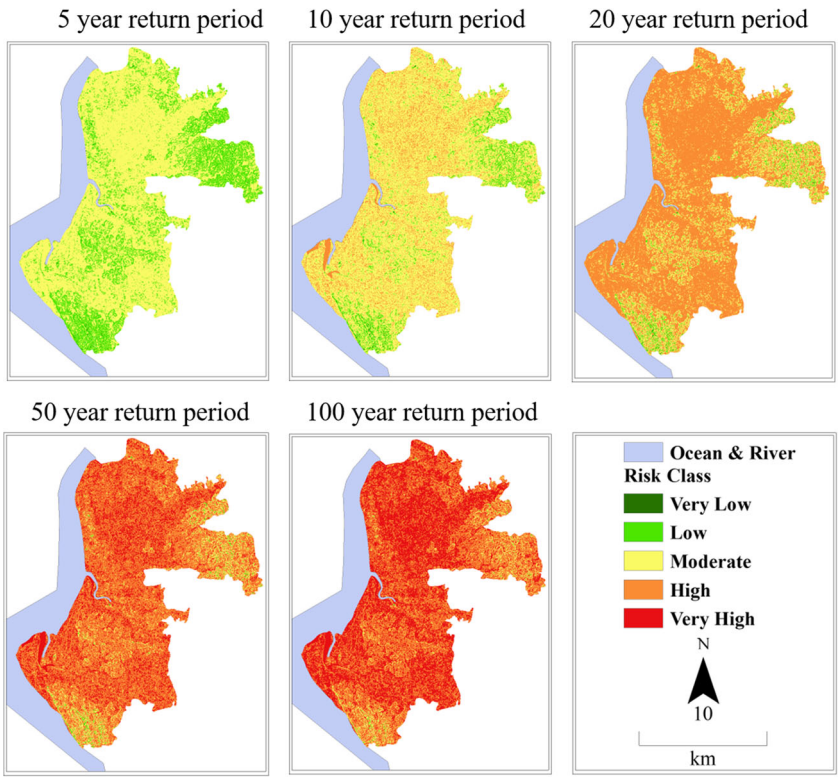

Fig. 15 Risk maps based on population for the present climate trend

Conclusion

Storm surges induced floods in the coastal areas of Bangladesh causes major problems in this era. With recent advancements in disaster management, the casualty due to cyclone is reduced but the loss and damages are still high in Bangladesh during a severe cyclone. In this research, an integrated risk-model was applied to determine the effects due to tropical cyclone-induced storm surge for the present and future climate conditions. This study aided with adopting spatial analysis based on primary and secondary data. The process was applied on the Cox's Bazar Sadar Upazilla on the Bangladesh coast, the geospatial linear storm-surge models were tested for this analysis. The storm surge models were reasonably applied in vulnerability and hazard assessment for the risk modeling using geospatial approaches. The geospatial methods were determined most likely effective for offering necessary spatial insights under the current approach. This strategy seemed to be effective while incorporate local understanding to develop precise and comprehensive information for future risks. Furthermore, in the risk modeling strategies intensive local climate change-based risk information modules are required. The overall efficiency of the model is encouraging and might be applied by coastal disaster supervision authorities to draw appropriate techniques and strategies to minimize surge effects. Thus, this research work would provide information for public work in the decision-making process during coastal management planning.

The study revealed that storm surge flooding forced hazards among the coastal community of Cox's Bazar Sadar Upazila. Moreover, future population growth, urbanization, sea-level rise could add higher risk and increases suffering among the community. Thus, a Decision Support System would be benefited from the risk zones identification in future development considerations for the Cox's Bazar Sadar Upazilla. With a proper dataset, this approach might be useful for other similar coasts around the world.

Acknowledgments The research was supported by the funds provided for **M**odeling **F**lood **I**nundation in a **C**oastal urban area (MFIC) research project (CUET/DRE/2017-18/CE/025), Chittagong University of Engineering and Technology (CUET), Bangladesh. We express our gratitude to the Cox's Bazar community, BWDB, CPA, BMD for providing bathymetric, meteorological, and validation data during the study.

References

BBS (Bangladesh Bureau of Statistics) (2011) Population and Housing Census 2011. Community Report: Chittagong. Ministry of Planning Statistics and Informatics Division, Dhaka, Bangladesh

Benson MA (1962) Evolution of methods for evaluating the occurrence of floods. Geol Surv Water-Supply Paper 1580-A. https://doi.org/10.3133/wsp1580A

Brammer H (2016) Floods, cyclones, drought and climate change in Bangladesh: a reality check. Int J Environ Stud 73(6):865–886. https://doi.org/10.1080/00207233.2016.1220713

Condon AJ, Sheng YP (2011) Evaluation of coastal inundation hazard for present and future climates. Nat Hazards 62:345–373. https://doi.org/10.1007/s11069-011-9996-0

Damen M, Van Westen CJ (1995) Modelling cyclone hazard in Bangladesh, pp 1–44. ILWIS Applications Guide. Available on: https://www.itc.nl/ilwis/pdf/appch03.pdf. Accessed June 2020

Darsan J, Asmath H, Jehu A (2013) Flood-risk mapping for storm surge and tsunami at Cocos bay (Manzanilla), Trinidad. J Coast Conserve 17:679–689. https://doi.org/10.1007/s11852-013-0276-x

Dasgupta S, Laplante B, Murray S, Wheeler D (2009) Climate change and the future impacts of storm-surge disasters in developing countries, Working Paper 182 September 2009. Cenrter for Global development (September 2009). Available on: https://www.cgdev.org/publication/climate-change-and-future-impacts-storm-surge-disasters-developing-countries-working

Dasgupta S, Huq M, Khan ZH, Ahmed MMZ, Mukherjee N, Khan MF, Pandey K (2014) Cyclones in a changing climate: the case of Bangladesh. Clim Dev 6:96–110. https://doi.org/10.1080/17565529.2013.868335

Dewan AM, Humayun Kabir M, Monirul Islam M, Kumamoto T, Nishigaki M (2007) Delineating flood risk areas in greater Dhaka of Bangladesh using geoinformatics. Georisk 1:190–201. https://doi.org/10.1080/17499510701772097

Emad M et al (2010) Global warming and hurricanes: the potential impact of hurricane intensification and sea level rise on coastal flooding intergovernmental panel on climate change. Climate Change, Springer 104:575–597. https://doi.org/10.1007/s10584-009-9790-0

Fang Y, Yin J, Wu B (2016) Flooding risk assessment of coastal tourist attractions affected by sea level rise and storm surge : a case study. Nat Hazards Springer Netherlands 84:611–624. https://doi.org/10.1007/s11069-016-2444-4

Gallant JC, Read AM, Dowling TI (2012) Removal of tree offsets from SRTM and other digital surface models. Int Arch Photagrammetry, Remote Sensings Patial Inform Sci. XXXIX(September):275–280

Gambolati G, Teatini P, Gonella M (2002) GIS simulations of the inundation risk in the coastal lowlands of the northern adriatic sea. Math Comput Model 7177(02):963–972

Hoque MM, Khan MSA (1996) Storm surge flooding in Chittagong city and associated risks. In: Destructive water: water-caused natural disasters, their abatement and control (Proceedings of the Conference held at Anaheim, California, June 1996). IAHS Publ. no. 239, 1997. Available on: http://hydrologie.org/redbooks/a239/iahs_239_0115.pdf. Accessed Nov 2020

Hoque MAA, Phinn S, Roelfsema C, Childs I (2017a) Modelling tropical cyclone risks for present and future climate change scenarios using geospatial techniques. Int J Digit Earth. https://doi.org/10.1080/17538947.2017.1320595

Hoque MAA, Phinn S, Roelfsema C, Childs I (2017b) Tropical cyclone disaster management using remote sensing and spatial analysis: a review. Int J Disaster Risk Reduct 22:345–354. https://doi.org/10.1016/j.ijdrr.2017.02.008

Karim FM, Mimura N (2008) Impacts of climate change and sea-level rise on cyclonic storm surge floods in Bangladesh. Global Environ Change 18:490–500. https://doi.org/10.1016/j.gloenvcha.2008.05.002

Khan SR (1991) Cyclone hazard in Bangladesh. Background Information on the Storm Surge Modelling. Available on: http://drm.cenn.org/Trainings; http://drm.cenn.org/Trainings/Multi%20Hazard%20Risk%20Assessment/Lectures_ENG/Session%2003%20Hazard%20assessment/Background/Coastal/Background_information_on_the_storm_surge_modelling%20in%20Bangladesh.pdf

Kumar A, Done J, Dudhia J, Niyogi D (2011) Simulations of cyclone Sidr in the bay of Bengal with a high-resolution model: sensitivity to large-scale boundary forcing. Meteorol Atmos Phys 114:123–137. https://doi.org/10.1007/s00703-011-0161-9

Lewis M, Bates P, Horsburgh K, Schumann G (2012) A storm surge inundation model of the northern bay of Bengal using publicly available data a bay of Bengal storm surge inundation model. Royal Meteorol Soc 358–369. https://doi.org/10.1002/qj.2040

Li D, Sun T, Liu M, Wang L, Gao Z (2016) Changes in wind speed under heat waves enhance urban heat islands in the Beijing metropolitan area. J Appl Meteorol Climatol 55:2369–2375. https://doi.org/10.1175/JAMC-D-16-0102.1

Li K, Li GS (2013) Risk assessment on storm surges in the coastal area of Guangdong Province. Nat Hazards 68(2):1129–1139. https://doi.org/10.1007/s11069-013-0682-2

Masood M, Takeuchi K (2011) Assessment of flood hazard, vulnerability and risk of mid-eastern Dhaka using DEM and 1D hydrodynamic model. Nat Hazards 61:757–770. https://doi.org/10.1007/s11069-011-0060-x

Mendelsohn R, Emanuel K, Chonabayashi S (2011) The impact of climate change on global tropical storm damages. Policy Research Working Paper Series 5562. The World Bank

Paul BK, Rashid H (2016) Climatic Hazards in Coastal Bangladesh-Non-Structural and Structural Solutions, p 342. https://doi.org/10.1016/C2015-0-00129-0

Peduzzi P, Chatenoux B, Dao H, de Bono A, Herold C, Kossin J, Mouton F, Nordbeck O (2012) Global trends in tropical cyclone risk. Nat Clim Change. Nat Publ Group 2(4):289–294. https://doi.org/10.1038/nclimate1410

Puotinen ML (2007) Modelling the risk of cyclone wave damage to coral reefs using GIS: a case study of the Great Barrier Reef, 1969–2003. Int J Geograph Inform Sci 21:97–120. https://doi.org/10.1080/13658810600852230

Saxena S et al (2012) Coastal hazard mapping in the Cuddalore region, South India. Nat Hazards 66:1519–1536. https://doi.org/10.1007/s11069-012-0362-7

Shepard CC, Agostini VN, Gilmer B, Allen T, Stone J, Brooks W, Beck MW (2012) Assessing future risk: quantifying the effects of sea level rise on storm surge risk for the southern shores of Long Island, New York. Nat Hazards 60:727–745. https://doi.org/10.1007/s11069-011-0046-8

Shultz JM, Russell J, Espinel Z (2005) Epidemiology of Tropical Cyclones : The Dynamics of Disaster , Disease , and Development. Johns Hopkins Bloomberg School of Public Health 27:21–35. https://doi.org/10.1093/epirev/mxi011

Shutler JD, Land PE, Piolle JF, Woolf DK, Goddijn-Murphy L, Paul F, Girard-Ardhuin F, Chapron B, Donlon CJ (2016) FluxEngine: a flexible processing system for calculating atmosphere-ocean carbon dioxide gas fluxes and climatologies. J Atmos Ocean Technol 33:741–756. https://doi.org/10.1175/JTECH-D-14-00204.1

Stedinger JR, Vogel RM, Georgiou EF (1993) Frequency analysis of extreme events. In: Maidmen DR (ed) In handbook of hydrology, vol 08. McGraw-Hill, New York, pp 18.1–18.66. https://doi.org/10.4236/me.2017.81006

Swinkels CM, Jeuken CMCJL, Wang ZB, Nicholls RJ (2009) Presence of connecting channels in the Western Scheldt estuary. J Coast Res 25:627–640. https://doi.org/10.2112/06-0719.1

Thompson CM, Frazier TG (2014) Deterministic and probabilistic flood modeling for contemporary and future coastal and inland precipitation inundation. Appl Geography 50:1–14. https://doi.org/10.1016/j.apgeog.2014.01.013

Ward P, Marfai M, Yulianto F, Hizbaron D, Aerts J (2011) Coastal inundation and damage exposure estimation: a case study for Jakarta. Nat Hazards 56(3):899–916

Weinkle J, Malue R, Pielke R Jr (2012) Historical global tropical cyclone landfalls. Am Meteorol Soc 25:4729–4735. https://doi.org/10.1175/JCLI-D-11-00719.1